Al-Azhar University Journal
for Virus Research and Studies

# Prelaminar Neuronal Tissue Thickness May Be the Solution

**Mona Elsayed Aly Hassan*[1]**

**[1]Department of Ophthalmology, Faculty of Medicine for Girls, Al-Azhar University,Cairo, Egypt**

***E-mail: Dr_Mona1408@hotmail.com**

## Abstract

This paper develops a new structural tool by enhanced depth imaging-optical coherence tomography (EDI-OCT) that enhances diagnosis of optic neuronal integrity in cases of anatomically disturbed optic nerve head. A prospective observational cross-sectional study included 66 subjects (66 eyes), 32 normal optic nerve head (group A), and 34 abnormal optic nerve head (group B), chosen from Al-Azhar University Hospitals and charity eye centre (El-Mustafa Eye Centre), from August 2022 to December 2022. They were investigated by perimetry, circumpapillary retinal nerve fiber (cpRNFL) scan, and enhanced depth imaging of optic nerve head scan by the spectralis OCT. The cpRNFL thickness was automatically segmented and calculated, while pre-laminar neuronal tissue thickness in enhanced depth images was segmented and calculated manually by built-in calibre software in spectralis OCT. There were a highly statistically significant positive correlation between Global circumpapillary RNFL thickness (94.94±17.91 um) and Prelaminar neuronal tissue thickness (96.19±18.06 um), with ($r=0.978$ and $p<0.001$); in normal optic nerve head group. There is no statistically significant negative correlation between Global circumpapillary RNFL thickness (102.88±19.90 um) and Prelaminar neuronal tissue thickness (91.53±22.83 um), with (r-0.241 and $p>0.05$); in abnormal optic nerve head group. A new EDI-OCT tool can extend our ability to measure prelaminar neuronal tissue thickness instead of cpRNFLT, for diagnosis and follow up for any neuropathy in abnormal ONH.

**Keywords:** Glaucoma, EDI-OCT, prelaminar neuronal tissue.

## 1. Introduction

The retinal nerve fiber layer (RNFL) consists of the retinal ganglion cell (RGC) axons, and Müller processes (ensheathe the neighbouring fibers, forming bundles) [1]. The peripapillary, or circumpapillary area denotes area adjacent to and including the optic nerve head. No clear cut-off of this area. Most of the morphometric and optical coherence tomography (OCT) studies have considered that; the circumpapillary retinal nerve fiber thickness (cpRNFL) area is a circle with radius of ± 3.5 mm. Some OCT devices consider cpRNFL area is a square (6×6 mm) around optic nerve head (ONH) [2]. All visual afferents, originating in the photoreceptor layer occupying more than 1000 mm 2 retina, are going to be on an area of about 2-3 mm2. So, cpRNFL thickness can provide data on focal loss, and hence on focal ganglion cells loss [3]. The neuroretinal tissue thickness is valuable in diagnosis and follow-up of

glaucoma, and other optic neuropathies. This is done conventionally by spectral domain optical coherence tomography (SD-OCT) cpRNFLT where zero delay at viteroretinal interface and automated segmentation. Automated segmentation depends on interference where the anterior border of RNFL is internal limiting membrane (ILM) and posterior border is ganglion cell layer (GCL) reflection in area around ONH [4]. The evidence-based literatures about bias of automated segmentations carry questions about accuracy and perfection of SD-OCT cpRNFLT in diagnosis and follow up of glaucoma and neurological disease. Large optic nerve, ONH drusen, parapillary optic atrophy, posterior vitreous detachment (PVD), tilted disc, congenital disc anomalies, epiretinal membrane, high myopia, bad centration all lead to failure of true automated segmentation [5-10]. Before making diagnostic decisions based on conventional printout of RNFL thickness, ophthalmologists should note if the patient has any abnormal ONH that may cause OCT artefacts and affect RNFL thickness interpretations. **So, we should ask: what's the solution?** Some authors found solution in macular ganglion cell complex (GCC). However, common reliability bias, as cpRNFL scan, includes signal quality and image artefact. Any coexisting macular disease may affect GCC thickness. In addition, most GCC scans cover a 6 x 6 mm; (20.8 degree of visual field), so patients who present with RNFL defect outside of this area may escape. The classic example is nasal step that may be present without OCT GCC defect [11]. Other authors try to develop combined structural algorithms to enhance cpRNFLT accuracy. The example of this is early glaucoma discrimination index (EGDI) that combines 4 tools; global RNFLT, inferior quadrant, inferotemporal clock hour, and absolute inter-eye inferior quadrants asymmetry [12]. The appearance of software in SD-OCT, that uses zero delay in chorioretinal junction, was first reported by Spaide et al, as enhanced depth imaging (EDI) [13]. Using this technique, the investigator can enhance ONH analysis by using Bruch's membranae opening – minimal rim width (BMO-MRW), lamina cribrosa (LC), LC pores, and peripapillary choroidal thickness in clinical diagnosis of glaucoma [14]. None had used EDI-OCT parameters in neurological disease till now. Few authors investigate prelaminar neuronal tissue thickness (PLNTT) and relation to visual function and perimetry mean deviation [15]. But no one could investigate the correlation between PLNTT and cpRNFLT in normal and abnormal appearance ONH. The aim of this study that investigate this correlation and its accuracy in both groups.

## 2. Patients and Methods

A prospective, observational, cross-sectional study included a total of 32 eyes of 32 subjects with normal appearance of optic nerve head (Group A), and 34 eyes of 34 subjects with abnormal optic nerve head (Group B). The study subjects were patients at ophthalmology department in Al-Azhar university hospitals and charity eye centre (El-Mustafa Eye Centre), from August 2022 to December 2022. The study was approved by the Ethics Committee of the Faculty of Medicine for Girls, Al-Azhar University. Written consent was taken from each participant in this study. All investigations were done in adherence to the Declaration of Helsinki. All patients were examined by systematic approach of ophthalmology as regard refraction by autorefractometer, best corrected visual acuity by Landolt chart at 6 meters and conversion of results to decimals for statistical purpose, optic nerve function clinical tests, Intraocular pressure (IOP) measurement by Goldmann applanation tonometry, anterior segment and posterior segment by slit lamp biomicroscopy. Optic nerve head is evaluated after pupil dilatation by Volk 90 D lens. Those with refraction < - 6 D and normal appearance

of optic nerve head was classified as **group A**. Those with spherical errors > - 6 D or abnormality in appearance of optic nerve head were classified as **group B**. Abnormal appearance of ONH is ONH that may influence the automated segmentation of cpRNFL by SD-OCT. It includes congenital anomalies as optic pit, tilted disc, myelinated nerve fiber layer, Bergmeister's papilla; or pathological anomalies as epiretinal membrane, PVD, myopic crescent, parapapillary atrophy (PPA), staphyloma, optic head buried drusen, and optic atrophy (any type). Pathological cupping was not considered as anomaly that may affect automated segmentation of OCT. Glaucoma diagnosis in this study was already made based on clinical evaluation and 3 successive perimetries.

### 2.1 Optical coherence tomography (OCT) image technique

All patients had SD-OCT cpRNFL thickness measured using a circular pattern. The Spectralis OCT (SD-OCT; Spectralis, Heidelberg Engineering Co., Heidelberg, Germany) with eye tracking system, which reduces motion artefacts. However, centration of circle on ONH is done manually by the operator. The scan automatically generated a quality score in decibels (dB), and multiple frames at the same location are obtained to reduce signal noise. For a typical eye length, the circle would be approximately 3.5 mm. The Spectralis OCT software (version 6.0.9) allows for automatic segmentation of the anterior and posterior borders of the RNFL to calculate the RNFL thickness for the overall global and 4 quadrants.

Then, EDI mode was on. The ONH protocol of imaging was a 15° (vertically) × 10° (horizontally) rectangle. Accurate centration here is not mandatory. For LC visibility at the EDI OCT scans, we used black /white; instead of false colored photos by OCT software. Only good-quality images were considered for analysis, with a signal-to-noise ratio >25 dB as suggested by device manufacturer. The LC was defined as the distance between the anterior and posterior lines of the highly reflective area in ONH. The prelaminar neuronal tissue thickness (PLNTT) was measured by using the built-in software calliper in micrometre. The PLNTT was defined as the vertical line between the anterior PLNT surface and the anterior line of the LC. When vascular shadows masked LC or prelaminar tissue visualization, we used the closest temporal images of ONH; to avoid this artefact.

### 2.2 Statistical Analysis

Analysis of our results was by SPSS version 20.0 (SPSS Inc., Chicago, Illinois, USA). Quantitative data were expressed as mean± standard deviation (SD). Qualitative data were expressed as frequency and percentage.

**The following tests were done:**

- **Spearman's rank correlation coefficient (rs):** It was used to assess correlations between cpRNFLT and PLNTT in two groups.
- Value of "r" ranges from -1 to 1 0 = no linear correlation.
- 1 = positive correlation - 1= negative correlation
- ***Positive*** **=** Increase in the independent variable leads to increase in the dependent variable & ***Negative*****=** Increase in the independent variable leads to decrease in the dependent.
- **Scatter plot:** a graph in which the values of cpRNFLT and PLNTT are plotted along two axes, for correlation pattern. The confidence interval was set to 95% and the margin of error accepted was set to 5%.
- Probability (P-value):

  P $\leq$0.05 was considered significant.

  P $\leq$0.001 was considered as highly significant.

  P > 0.05 was considered insignificant.

## 3 .Results

Results of our study are the age ranged from 18 – 57 years with mean age (39.65 ± 11.31) they were 11 females (55.0%) and 9 males (45.0%). (Table 1). Table 1 shows higher percentage of female gender, about 45% of precipitants had pathological cupping with normal anatomical criteria of ONH. Data are expressed as Mean ±SD, & number (%). Table 2 shows high significant and positive correlation between Global circumpapillary RNFL thickness (um) and Prelaminar neuronal tissue thickness (um), with (r=0.978 and p<0.001). Spearman's rank correlation coefficient (rs) ** highly statistically significant correlation (p<0.001). Table 3 shows similar accuracy of prelaminar neuronal tissue measurement and circumpapillary retinal nerve fiber layer thickness in group A. Sens.: Sensitivity; PPV: Positive predictive value; FN: False Negative.

**Table (1):** Demographic and ophthalmic data among group A normal (n=32)..

| Variable | Group A Normal (n=32) |
|---|---|
| Gender | |
| Female | 24 (75.0%) |
| Male | 8 (25.0%) |
| Age (years) | |
| Mean ±SD | 49.44±15.06 |
| Range | 11_67 |
| Spherical Refraction | |
| Mean ±SD | 0.17±1.56 |
| Range | -2_3 |
| ONH anatomical appearance | |
| CUP | 14 (43.8%) |
| Normal | 18 (56.3%) |
| Glaucoma | |
| No | 20 (62.5%) |
| Yes | 12 (37.5%) |
| Global circumpapillary RNFL thickness (um) | |
| Mean ±SD | 94.94±17.91 |
| Range | 47_121 |
| Prelaminar neuronal tissue thickness (um) | |
| Mean ±SD | 96.19±18.06 |
| Range | 53_124 |

**Table (2):** Correlation between Global circumpapillary RNFL thickness and Prelaminar neuronal tissue thickness among group A normal.

| **Group A Normal** | **Global circumpapillary RNFL thickness (um)** | |
|---|---|---|
| | **Rs** | **p-value** |
| **Prelaminar neuronal tissue thickness (um)** | 0.978 | <0.001** |

**Table (3):** Demographic and ophthalmic data among group A normal (n=32).

| | | **Gold standard** | **Sens.** | **PPV** | **FN** | **Accuracy** |
|---|---|---|---|---|---|---|
| | | **Disease (n=12)** | | | | |
| Global circumpapillary RNFLT | Disease | 6 | 50% | 100% | 50% | 50% |
| | Not disease | 6 | | | | |
| Prelaminar neuronal tissue thickness | Disease | 6 | 50% | 100% | 50% | 50% |
| | Not disease | 6 | | | | |

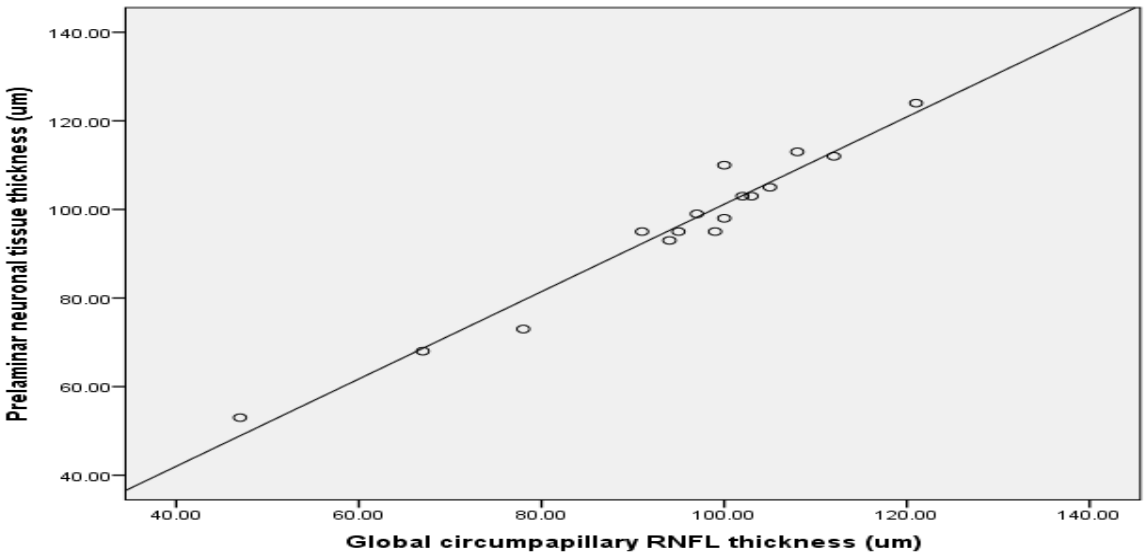


**Figure (1):** Scatter plot showing significant positive correlation between Global cpRNFL thickness (um) and Prelaminar neuronal tissue thickness (um).

**Table (4):** Different parameters distribution among group B abnormal (n=34).

| Variable | Group B Abnormal (n=34) |
|---|---|
| **Gender** | |
| Female | 20 (58.8%) |
| Male | 14 (41.2%) |
| **Age (years)** | |
| Mean ±SD | 40.18±16.26 |
| Range | 11_63 |
| **Spherical Refraction** | |
| Mean ±SD | -1.47±4.39 |
| Range | -13_2 |
| **ONH anatomical appearance** | |
| ONH Drusen | 12 (35.3%) |
| Temporal Pallor | 4 (17.6%) |
| Myopic Crescent, Tilted Disc | 6 (11.8%) |
| Tilted Disc | 4 (11.8%) |
| Epiretinal Membrane | 3 (5.9%) |
| Hypermetropic Disc | 1 (5.9%) |
| Optic Pit | 1 (5.9%) |
| Parapapillary Atrophy | 3 (5.9%) |
| **Glaucoma** | |
| No | 22 (64.7%) |
| Yes | 12 (35.3%) |
| **Global circumpapillary RNFL thickness (um)** | |
| Mean ±SD | 102.88±19.90 |
| Range | 87_157 |
| **Prelaminar neuronal tissue thickness (um)** | |
| Mean ±SD | 91.53±22.83 |
| Range | 31_125 |

Table 4 shows more or less same percentage female and male gender, about 35% of precipitants had pathological cupping with abnormal anatomical criteria of ONH. Data are expressed as Mean ±SD, & number (%). Table 5 shows there is no statistically significant and negative correlation between Global circumpapillary RNFL thickness (um) and Prelaminar neuronal tissue thickness (um), with (r-0.241 and p>0.05). Table 6 shows higher accuracy of prelaminar neuronal tissue measurement in group B. Sens.: Sensitivity; PPV: Positive predictive value; FN: False Negative. Table 6 shows higher accuracy of prelaminar neuronal tissue measurement in group B. Sens.: Sensitivity; PPV: Positive predictive value; FN: False Negative.

**Table (5):** Correlation between Global circumpapillary RNFL thickness and Prelaminar neuronal tissue thickness among group B abnormal.

| Group B Abnormal | Global circumpapillary RNFL thickness (um) | |
|---|---|---|
| | Rs | p-value |
| Prelaminar neuronal tissue thickness (um) | -0.241 | 0.351 |

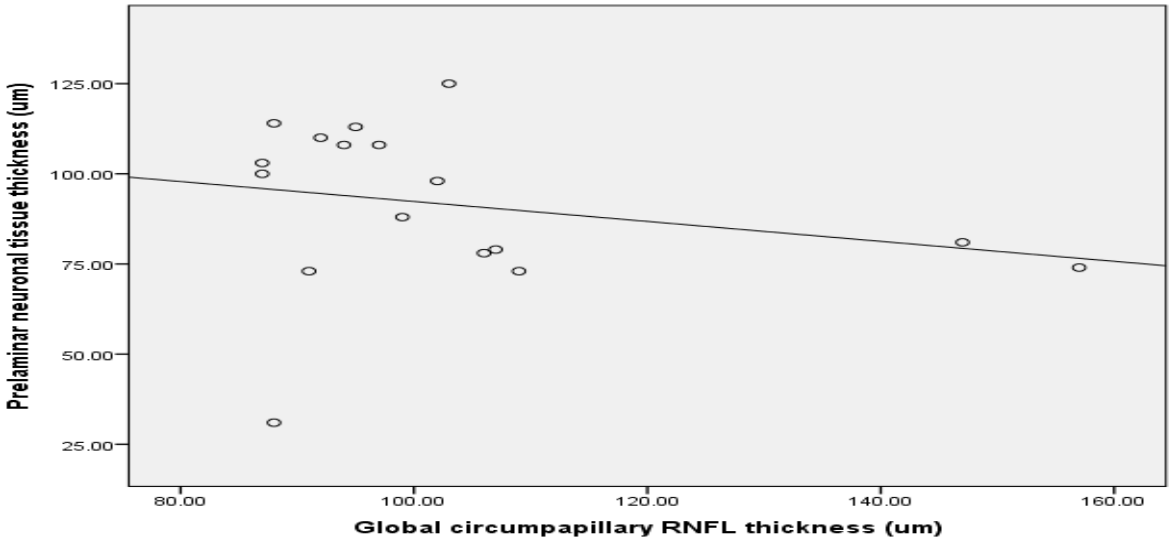


**Figure (2):** Scatter plot shows no statistically significant negative correlation between Global cpRNFL thickness (um) and Prelaminar neuronal tissue thickness (um).

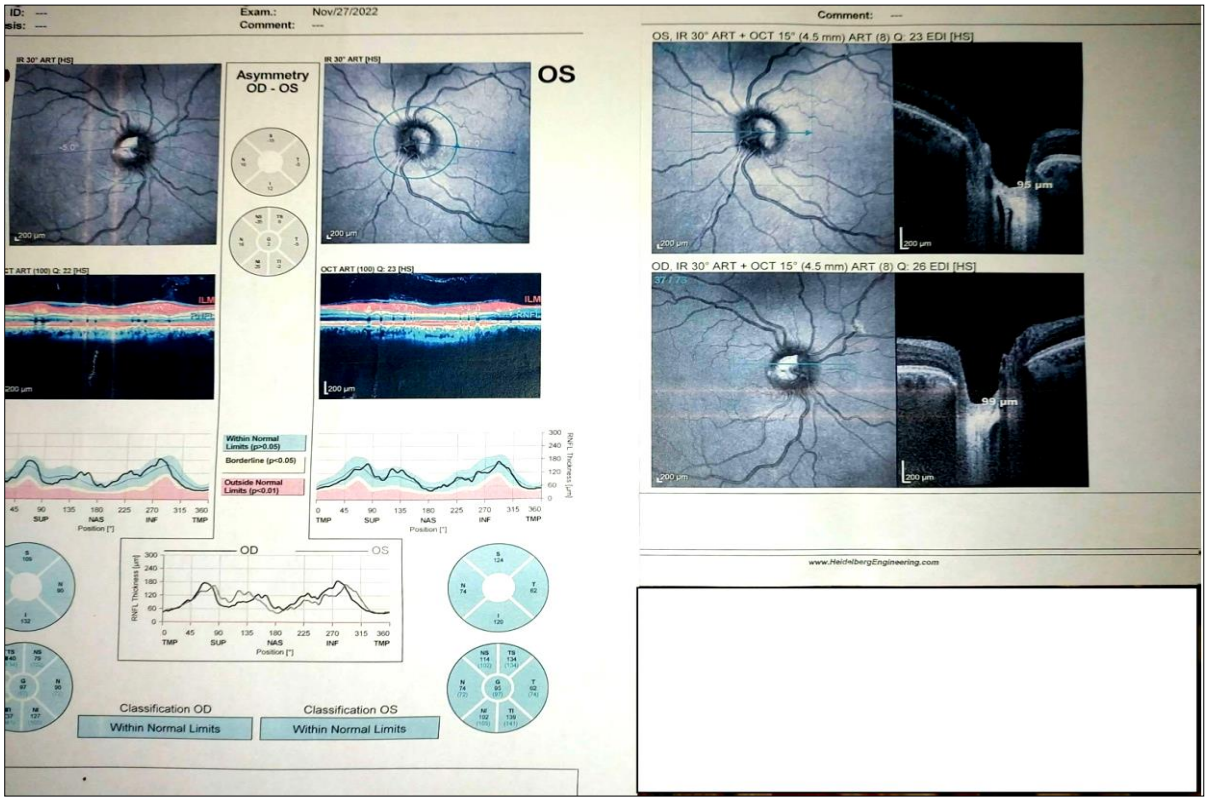


**Figure (3):** The normal optic nerve head as shown in en face red free image, the conventional cpRNFL, and PLNTT by EDI – OCT more or less the same value.

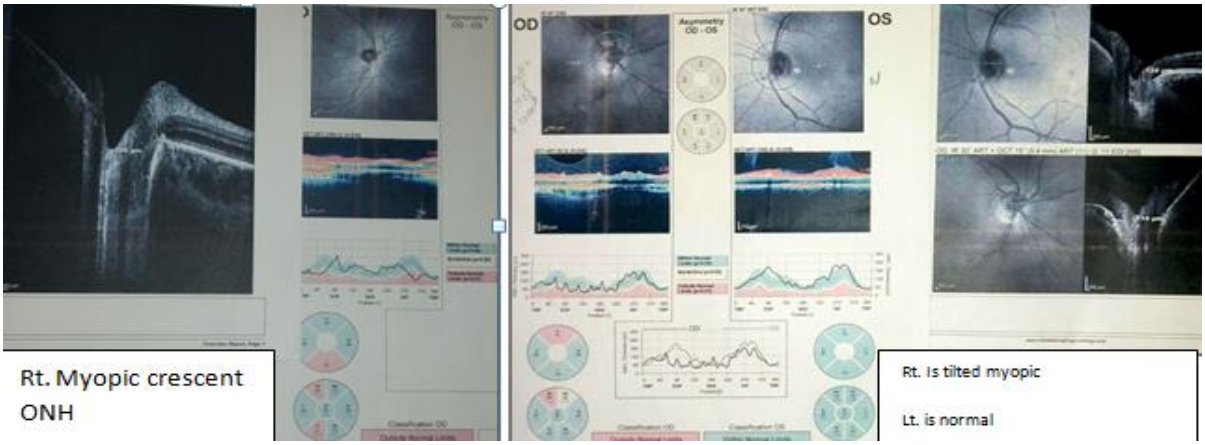


**Figure (4):** The abnormal optic nerve head (myopic crescent) as shown in en face red free image, the conventional cpRNFL, and PLNTT by EDI – OCT are not the same..

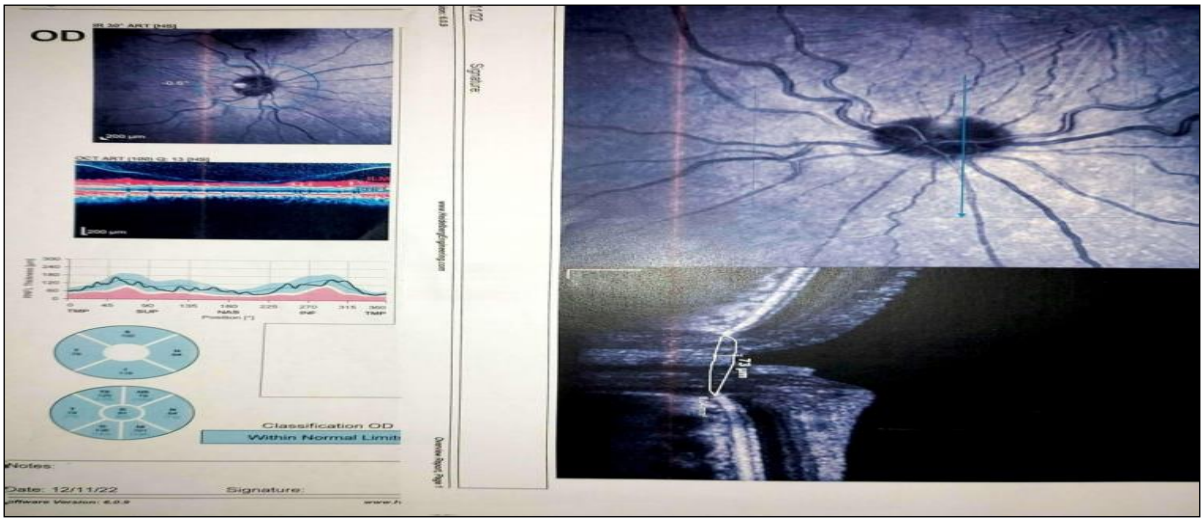


**Figure (5):** The abnormal optic nerve head (epiretinal membrane) as show in en face red free image, the conventional cpRNFL, and PLNTT by EDI – OCT are not the same.

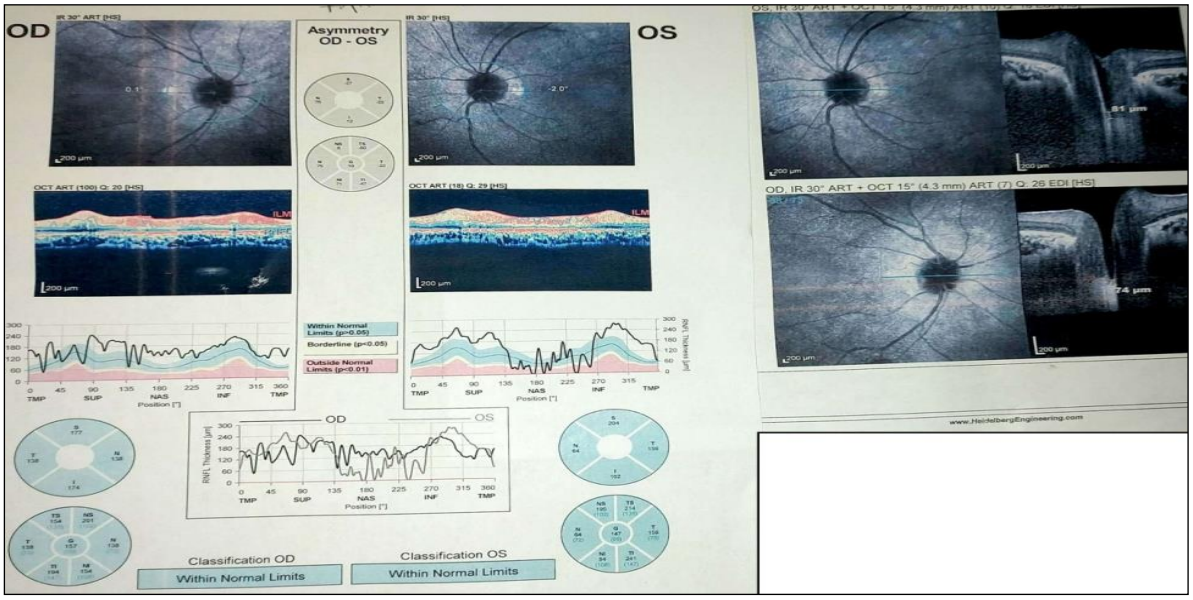


**Figure (6):** The abnormal optic nerve head (ONH drusen) as show in en face red free image, the conventional cpRNFL, and PLNTT by EDI – OCT are not the same.

## 3. Discussion

Many methods are established in enhancing performance of OCT in ONH structural integrity. Evolving automated segmentation software, true eye tracker, and 3D analysis are used in assessment of peripapillary RNFL. The old version of OCT devices has no automated segmentation. The automated segmentation even developed from depending on retinal pigment epithelium (RPE) as a border of ONH, to the concept of Bruch membrane opening (BMO). They automatically analyze the cp-RNFL thickness depending on minimal width from BM to ILM. This method has a higher diagnostic performance than classic cpRNFL; that depends on neuronal rim segmentation from ILM to GCL [16]. However, both methods have many artifacts. BMO-MRW has artifact of blood vessel location that led to overestimation of RNFL thickness [17]. So, the investigators should be aware of Blood vessel location and taken into consideration. Another issue is: still cannot solve problem of peripapillary chorioretinal atrophy as in myopes as they have wide BMO and false results [18]. Sung et al. [19] found variability in BMO in myopes with enlargement and thinning of BMO-MRW making diagnosis of glaucoma in myopes questionable. CpRNFLT by conventional automated segmentation has many artifacts. Liu et al. [8] investigated 2313 eyes with OCT cpRNFLT conventional method to seek for types of artifacts. They found 12 types of artifacts; and in about 46% of their eye scans. Artefacts include decentration, poor signals, poor automated anterior and posterior segmentation, myopia, PVD, epiretinal membrane, myelinated NFL, posterior staphyloma, end stage glaucoma, and PPA. Asrani et al. [20] found that 19.9% of RNFL scans contained artefacts, especially when epiretinal membranes were present. Han et al. [21] found error in identification of the anterior RNFL, false segmentation of the posterior RNFL, incomplete segmentation, decentred scans, and borders artefacts. In addition, we still worried about built-in normative data that labels the red disease based on ethnicity and age group only. This point is noted in both conventional segmentation and BMO-MRW. The correlation between cpRNFLT and BMO-MRW was studied. Gardiner et al. [22] published data that suggest BMO-MRW early detection of glaucomatous damage although cpRNFLT is valuable in glaucoma monitoring. The BMO-MRW elicits thinning before appearance of cpRNFLT thinning. ONH biomechanical studies found that the ONH is the place of damage beginning. Stress and strain caused by IOP within the ONH affect both nutrient and supply of blood to RGC axons even with absence of laminar deformation [23,24]. In early glaucoma, the neural canal may become enlarged and elongated, and prelaminar neural tissues become affected while retinal nerve fiber layer is not affected yet. In another word, cpRNFLT usually is measured distant from the ONH and may be less affected by such changes [25]. The researchers have been investigating new metrics based both on prelaminar neural tissue (PLNT) and laminar analyses [26-28]. The higher value of prelaminar neuronal tissue thickness (PLNTT) in early glaucoma diagnosis is evaluated and compared to conventional cpRNFL by Lopes et al. [15] in large study, recently.

To our knowledge, this is the first study that investigates the correlation between cpRNFLT ‘that automatically segmented’ and PLNTT ‘that manually segmented’ in both normal ONH and abnormal ONH. We assume that combining machine tool by OCT and human expert tool by manual segmentation will decrease the errors and artefacts in abnormal ONH. This is valuable in many diseases not only glaucoma but neurological. We found statistically significant positive correlation ($r=0.978$ and $p<0.001$) in normal ONH. This is making both methods are not different when we have normal posterior

neuronal opening of ONH. But no correlation (r-0.241 and p>0.05) between them in abnormal optic nerve head as epiretinal membrane, tilted disc, disc drusen, myopic cresent, ONH pit, PPA, temporal pallor, and hypermetropic disc. The diagnostic accuracy of PLNTT was 71.4 % versus 14.3 % for cpRNFLT in abnormal ONH. We introduced manual segmentation of PLNTT as the solution instead of conventional cpRNFLT in diagnosis and follow up, when the ONH is abnormal. We assume also; it may be better way than BMO-MRW as we can avoid artefacts "e.g., blood vessels shadowing, and chorioretinal atrophy that cannot be avoided by OCT machine".

## 4. Conclusion

A new EDI-OCT tool can extend our ability to measure prelaminar neuronal tissue thickness instead of cpRNFLT, for diagnosis and follow up for any neuropathy in abnormal ONH.

**Acknowledgment:** I would like to Acknowledge contributions made by Dr. Hend Mohammed Safwat in OCT imaging of patients in this study.

**Financial support:** Nil.

**Conflict of interest:** None.

## References

1. Airaksinen PJ, Doro S, and Veijola J (2008). Conformal Geometry of Retinal Nerve Fiber Layer. Proceedings of National Academy of Science (PANS); 105: 19690-19695.

2. Ditchl A, Jonas JB, and Naumann GOH (1999). Retinal Nerve Fiber Layer in Human Eyes. Graefe's Arch Clin Exp ophthalmol; 237: 474- 479.

3. Frenkel S, Morgan JE, and Blumenthal EZ (2005). Histological Measurement of Retinal Nerve Fibre Layer Thickness. Eye; 19: 491-498.

4. Meier KL, Greenfield DS, Hilmantel G, et al. (2014). Special commentary: Food and Drug Administration and American Glaucoma Society Co-Sponsored Workshop: the validity, reliability, and usability of glaucoma imaging devices. Ophthalmology; 121: 2116-2123.

5. Chang RT and Singh K (2013). Myopia and glaucoma: diagnostic and therapeutic challenges. Curr Opin Ophthalmol; 24(2):96–101.

6. Francisconi CLM, Wanger MB, RibeiroRVP et al. (2020). Effects of axial length on retinal nerve fiber layer and macular ganglion cell-inner plexiform layer measured by spectral-domain OCT. Arq Bras of Ophthalm. [online]; v. 83, n. 4 [Accessed 1 December 2022], pp. 269-276.

7. Nana Wandji B, Dugauquier A, Ehongo A (2022). Visual field defects and retinal nerve fiber layer damage in buried optic disc drusen: a new insight. Int J Ophthalmol;15(10):1641-1649.

8. Liu Y, Simavli H, Que CJ, et al. (2015). Patient characteristics associated with artifacts in Spectralis optical coherence tomography imaging of the retinal nerve fiber layer in glaucoma. Am J of Ophthalmol;159 (3):565-76. e2.

9. LeshnoA, Hood DC, Liebmann JM, De Moraes CG (2022). Identifying and understanding optical coherence tomography artifacts that may be confused with glaucoma. Rev Bras Oftalmol; 81: e0103.

10. Bayer A and Akman A (2020). Artifacts and Anatomic Variations in Optical Coherence Tomography. Turk J Ophthalmol; 50:99-106.

11. Bruce AS and Huang I (2014). What Is the Earliest Test for Glaucoma? Use of Ganglion Cell Complex as A New Diagnostic Indicator. PHarma; 3: 8-10.
12. Safwat H, Nassar E, Rashwan A (2020). Early Glaucoma Discrimination Index. J Curr Glaucoma Pract;14(1):16–24.

13. Spaide RF, Koizumi H, Pozzoni MC (2008). Enhanced depth imaging spectral-domain optical coherence tomography. Am J Ophthalmol;146(4):496-500.

14. Gmeiner JM, Schrems WA, Mardin CY, et al. (2016). Comparison of Bruch's membrane opening minimum rim width and peripapillary retinal nerve fiber layer thickness in early glaucoma assessment. Invest Ophthalmol Vis Sci; 57(9): OCT575–84.

15. Lopes FSS, Matsubara I, Almeida I, et al. (2021). Using Enhanced Depth Imaging Optical Coherence Tomography-Derived Parameters to Discriminate between Eyes with and without Glaucoma: A Cross-Sectional Comparative Study. Ophthalmic Res64:108-115.

16. Chauhan BC, Danthurebandara VM, Sharpe GP, et al. (2015). Bruch's Membrane Opening Minimum Rim Width and Retinal Nerve Fiber Layer Thickness in a Normal White Population: A Multicenter Study. Ophthalmology; 122(9):1786–1794.

17. La Bruna S, Tsamis E, Zemborain ZZ, et al. (2020). A Topographic Comparison of OCT Minimum Rim Width (BMO-MRW) and Circumpapillary Retinal Nerve Fiber Layer (cRNFL) Thickness Measures in Eyes with or Suspected Glaucoma. J Glaucoma;29(8):671-680.

18. Yu Sawada, Makoto Araie, Hitomi Shibata, et al. (2019). Differences in Retinal Nerve Fiber Layer Thickness as Assessed on the Disc Center and Bruch's Membrane Opening Center in Myopic Eyes. Ophthalmology Glaucoma; 2(3): 2019, 145-155.

19. Sung MS, Heo MY, Heo H, Park SW (2019). Bruch's membrane opening enlargement and its implication on the myopic optic nerve head. Sci Rep; 9(1):19564.

20. Asrani S, Essaid L, Alder BD, Santiago-Turla C (2014). Artifacts in Spectral-Domain Optical Coherence Tomography Measurements in Glaucoma. JAMA Ophthalmol; 132(4):396.

21. Han IC and Jaffe GJ (2010). Evaluation of artifacts associated with macular spectral-domain optical coherence tomography. Ophthalmology;117(6):1177–1189.

22. Gardiner S, Boey P, Yang H, et al. (2015). Structural measurements for monitoring change in glaucoma: comparing retinal nerve fiber layer thickness with minimum rim width and area: Structural measurements of change in glaucoma. Invest Ophthalmol Vis Sci; 56:6886–6891.

23. Burgoyne CF (2011). A biomechanical paradigm for axonal insult within the optic nerve head in aging and glaucoma. Exp Eye Res; 93:120–132.

24. Park K, Kim J, Lee J (2018). The Relationship Between Bruch's

Membrane Opening-Minimum Rim Width and Retinal Nerve Fiber Layer Thickness and a New Index Using a Neural Network. Transl Vis Sci Technol; 7(4):14.

25. Yang H, Downs J, Girkin C, et al. (2007). 3-D histomorphometry of the normal and early glaucomatous monkey optic nerve head: Lamina cribrosa and peripapillary scleral position and thickness. Invest Ophthalmol Vis Sci; 48:4597–4607.

26. Barrancos, C., Rebolleda, G., Oblanca, N. et al. (2014). Changes in lamina cribrosa and prelaminar tissue after deep sclerectomy. Ey; 28: 58–65.

27. Prata TS, Lopes FS, Prado VG, et al. (2017) In vivo analysis of glaucoma-related features within the optic nerve head using enhanced depth imaging optical coherence tomography. PLoS ONE; 12(7): e0180128.

28. Ersöz MG, Kunak Mart D, Hazar L, et al. (2018). Evaluation of Prelaminar Region and Lamina Cribrosa with Enhanced Depth Imaging Optical Coherence Tomography in Pseudoexfoliation Glaucoma. Turk J Ophthalmol; 48(3):109-114.